Physical Layer Network Coding with Signal Alignment for MIMO Wireless Networks

Ruiting Zhou†, Zongpeng Li†, Chuan Wu‡, Carey Williamson†
† Department of Computer Science, University of Calgary, {*rzho, zongpeng, carey*}*@ucalgary.ca*
‡ Department of Computer Science, University of Hong Kong, *cwu@cs.hku.hk*

***Abstract*—We propose signal alignment (SA), a new wireless communication technique that enables physical layer network coding (PNC) in multi-input multi-output (MIMO) wireless networks. Through calculated precoding, SA contracts the perceived signal space at a node to match its receive diversity, and hence facilitates the demodulation of linearly combined data packets. PNC coupled with SA (PNC-SA) has the potential of fully exploiting the precoding space at the senders, and can better utilize the spatial diversity of a MIMO network for higher transmission rates, outperforming existing techniques including MIMO or PNC alone, interference alignment (IA) and interference alignment and cancellation (IAC). PNC-SA adopts the seminal idea of *'demodulate a linear combination'* from PNC. The design of PNC-SA is also inspired by recent advances in IA, though SA aligns *signals* not *interferences*. We study the optimal precoding and power allocation problem of PNC-SA, for SNR maximization at the receiver. The mapping from SNR to BER is then analyzed, revealing that the throughput gain of PNC-SA does not come with a sacrifice in BER. We finally demonstrate general applications of PNC-SA, and show via network level simulations that it can substantially increase the throughput of unicast and multicast sessions, by opening previously unexplored solution spaces in multi-hop MIMO routing.**

I. Introduction

New physical layer techniques and their applications in wireless routing have been active areas of research in the recent past. A salient example is multi-input multi-output (MIMO) communication. A MIMO link employs multiple transmit and receive antennas that operate over the same wireless channel. MIMO transmission brings extra spatial diversity that can be exploited to break through capacity limits inherent in single-input single-output (SISO) channels [1], [2]. Another recent example is physical layer network coding (PNC) [3], which extends the concept of network coding [4] from higher layers to the physical layer. PNC is seminal in that it utilizes the natural additive property of E-M waves in space. Viewing collided transmissions simply as superimposed signals, PNC applies tailored demodulation for translating them into linear combinations of transmitted data packets. Such demodulated linear combinations, similar to encoded packets in network coding [4], are then used to facilitate further data routing.

We propose signal alignment (SA), a new technique that enables PNC in wireless networks consisting of MIMO links. A central idea behind SA is to improve network capacity by enabling simultaneous transmissions from multiple MIMO senders. SA performs calculated precoding at the senders, such that the number of dimensions spanned by signals arriving at a receiver is reduced to exactly match its receive diversity. Consequently, the receiver can decode linear combinations of the transmitted packets. This is through classic MIMO detection, such as maximum likelihood detection (ML) or zero forcing (ZF) [1], [5], followed by PNC mapping [3]. In this paper, we demonstrate that PNC coupled with SA (PNC-SA) can open new solution spaces for routing in MIMO networks, leading to higher throughput with good bit-error-rate (BER), as compared to previous techniques.

The idea and benefit of PNC-SA can be illustrated in an uplink communication scenario, designed to motivate interference alignment and cancellation (IAC) [2], a recent technique for improving throughput in MIMO networks. PNC-SA provides a further throughput gain over IAC at 33%, under high SNR.

Fig. 1 depicts the MIMO uplink from two clients to two APs. Each node is equipped with 2 antennas that operate at the same channel, with flat Rayleigh fading [1], [2]. During propagation, a signal experiences amplitude attenuation and phase shift, which can be modeled using a complex number. $\mathbf{H_{ij}}$ is the 2×2 complex matrix for the channel gains from client i to AP j. An Ethernet link connects the two APs, enabling limited collaboration: digital packets can be exchanged, but not analog ones [2]. The goal is to send packets from the clients to the APs as fast as possible.

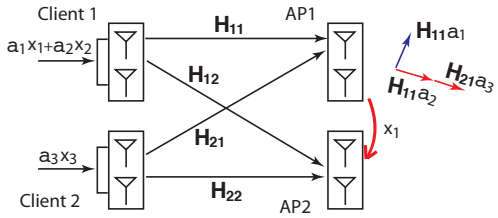

Fig. 1. The 2-client 2-AP MIMO uplink. IAC achieves a throughput of 3 packets per time unit. Each $\mathbf{a_i}$ is a 2×1 precoding vector. $\mathbf{H_{11}a_1}$ is called the *direction* of x_1 at AP1.

A naive solution uses one send-receive antenna pair to avoid any interference at all. Let's normalize a time unit to be one packet transmission time here. For a quick improvement, we can use a 2×2 MIMO link formed by a client-AP pair, to transmit two packets, x_1 and x_2, simultaneously. The AP receives two overlapped signals of x_1 and x_2. ML or ZF detection can be applied to recover x_1 and x_2, increasing the throughput from 1 to 2 packets (per time unit).

Can we utilize all available antennas to form a 4×4 MIMO

link, to transmit >2 packets? The answer is, unfortunately, 'no'. As the four receive antennas are distributed at two nodes, we do not have all four received analog signals at one location, as required in MIMO decoding.

IAC breaks through this bottleneck by combining interference alignment (IA) and interference cancellation (IC) techniques. As shown in Fig. 1, IAC first performs precoding over 3 packets x_1, x_2 and x_3 at the clients, such that x_2 and x_3 arrive along the same direction at AP1. *Direction* here is an abstract contract defined as a signal's encoding vector when received at AP1. AP1 has two equations and two unknowns, from which it can solve x_1. Next, AP1 transmits x_1 in digital format to AP2. AP2 subtracts the component of x_1 from its received signals, leaving it with two equations and two unknowns, from which it recovers x_2 and x_3.

Can we use IAC to transmit 4 packets instead of 3, in one time unit? The answer is 'no'. With IAC, the intended signal has to take its own direction at AP1, while all other 'interferences' take another. As a result, the two packets from client 2 has to be aligned to the same direction at AP1. This requires identical precoding vectors for them, making them impossible to separate at AP2.

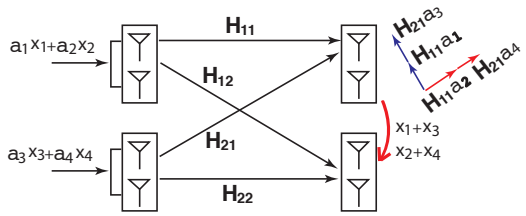

Fig. 2. PNC-SA can achieve a throughput of 4 packets per time unit.

Departing from such a requirement of IA and IAC, SA allows multiple *signals* to be aligned to the same direction at a receiver. In fact, there is no *interference* in SA; all packet transmissions are treated as *signals*. As shown in Fig. 2, PNC-SA simultaneously transmits 4 packets, $x_1, \ldots, x_4$. Precoding is performed such that at AP1, x_1 and x_3 are aligned to the same direction, and the same for x_2 and x_4. AP1 has two equations and two unknowns (x_1+x_3, x_2+x_4), from which it solves x_1+x_3, x_2+x_4 to transmit in digital format to AP2. Having accumulated 4 equations, AP2 then solves them to recover the 4 original packets, $x_1, \ldots, x_4$.

Two ideas work in concert with each other in the PNC-SA solution. One is *demodulating a linear combination*, adapted from PNC. The other is *precoding at sender for alignment at receiver*, inspired by IA. PNC-SA helps the exploration of the full precoding space at the senders, and the full spatial diversity of the system. As we will show, PNC and IAC can indeed be viewed as special cases of PNC-SA. When each node has a single receive diversity, SA degrades into phase synchronization [3], [6], and PNC-SA degrades into PNC. With extra restrictions on precoding and decoding, PNC-SA degrades into IAC.

In wireless transmissions, throughput improvement is less attractive if it comes with higher BER. The BER of the PNC-SA scheme depends on two factors: (a) the SNR at the receiver, and (b) BER as a function of SNR. While (a) depends on precoding (signal pre-rotation and power allocation) at senders, (b) depends on the modulation scheme. We study each factor in detail. We show that SA introduces a new, interesting optimization problem in precoding design, and classic solutions such as singular value decomposition followed by water filling (SVD-WF) does not apply any more. We formulate the optimization as a vector programming problem, and design an efficient solution using orthogonal signal alignment. The SNR-BER performance of PNC-SA is then analyzed, and compared to that of IAC. We observe that the throughput gain of PNC-SA indeed does not come with a cost in error rate.

The application of PNC-SA is not limited to scenarios of limited receiver collaboration. We study general applications of PNC-SA in multi-hop MIMO networks, for routing tasks including information exchange, unicast, and multicast/broadcast. We show that PNC-SA opens previously unexplored solution spaces for MIMO routing, and can augment the capacity region of a MIMO network. Via packet-level simulations, throughput gains of up to $2\times$ are observed, especially at high SNR. In both unicast and multicast routing, PNC-SA can lead to a natural fusion of PNC and digital network coding (DNC).

In the rest of the paper, we review previous research in Sec. II, and outline the system model and assumptions in Sec. III. We present a detailed PNC-SA solution in Sec. IV, and analyze its BER performance in Sec. V. Sec. VI presents general applications of PNC-SA in multi-hop routing, and packet level simulations. Sec. VII concludes the paper.

II. Previous Research

Cadambe and Jafar [7] studied interference alignment for k node pairs, communicating over the same channel. They demonstrated that such a system allows $k/2$ degrees of freedom. Intuitively, if a single node pair can communicate at rate C, then the k pairs can simultaneously communicate at a rate of $C/2$ each. This discovery of *everyone gets half of the pie* has since spurred considerable interest in the wireless communication community. The underlying technique, aligning unwanted signals and contracting their dimensions perceived at a receiver, has spawned further applications [2], [8], [9]. Our SA proposal was inspired by the same idea. However, SA does not necessarily differentiate between *wanted signals* and *unwanted interferences*. Correspondingly, in SA, there is usually no single signal of focus, which requires demodulation in uncoded form.

Gollakota *et al*. [2] combined IA with IC in their IAC scheme, tailored for the scenario of multi-user MIMO transmission with limited receiver collaboration. One of the receivers has its 'interferences' aligned, and one or more original packets demodulated (IA). The demodulated packets are then sent in digital form to another receiver to help further decoding (IC). Li *et al*. [8] studied the application of IAC in more general, multi-hop wireless networks. The problem of appropriately applying IAC across a network is formulated

and solved through a convex programming approach. Unlike PNC-SA, IA and IAC demodulate original packets but not their linear combinations. The IA phase in IAC can be viewed as a special case of PNC-SA precoding, and the IC phase is a special case of *decoding via remodulation* in PNC-SA (Sec. IV).

MIMO transmission has proven promising for providing spatial diversity and power gains that lead to high transmission rates, over a single wireless channel [1], [10]. Compared to a traditional SISO link, a $k\times k$ MIMO link can provide up to $k\times$ capacity gain at all SNR [1]. Given a MIMO channel with full CSI, the precoding at the sender computes pre-rotations of source signals and power allocation among them, to maximize overall channel capacity. A classic technique is to apply singular value decomposition to obtain the eigenmode channel decomposition, where the MIMO channel is transformed into a set of independent virtual SISO channels. Then water filling (WF) is applied to gradually allocate power to the virtual channels, giving priority to the one with current highest marginal capacity gain [1]. However, WF fails to work for the new precoding problem introduced by PNC-SA, due to the presence of the extra alignment constraint.

Zhang *et al*. [3] initiated the study of physical layer network coding, where entangled E-M signals are viewed as new, linearly combined packets. Using the 3-node Alice-and-Bob example for information exchange, Zhang *et al*. showed how a PNC-demodulation algorithm can be implemented at the relay, to extract the digital version of p_a (packet from Alice) xor p_b (packet from Bob). PNC is new both in utilizing collided transmissions as useful encoded signals, and in demodulating a linear combination of transmitted packets. Zhang and Liew further studied PNC in the Alice-and-Bob scenario with two antennas at the relay [11]. They examined how the two different combinations at the relay can be exploited to improve the BER of PNC. We show in Sec. VI-A that when all nodes have multiple antennas, PNC-SA is required to utilize the full spatial diversity of the network.

A previous work, MIMO compute-and-forward [12], studies the theoretical achievable rates of a many-to-one transmissions, with multiple antennas at each node. Assuming all senders employ the same lattice code for modulation, the authors demonstrate that the idea of demodulating a linear combination from PNC can improve the achievable rates. They also point out the importance of optimal precoding at the senders, but leave such non-convex optimization as an open problem. In this paper, the optimal precoding problem of PNC-SA is formulated and solved in Sec. IV.

III. Model and Notation

We consider a multi-hop wireless network where each node is equipped with one or more antennas. Flat Rayleigh channel fading [1], [2], [8] is assumed, in which a signal experiences amplitude attenuation and phase shift through a channel. In each one-hop transmission, the sender transmits an N_t-dimensional signal vector $\mathbf{x}$, using the same carrier frequency. The receiver records an N_r-dimensional complex signal vector $\mathbf{y} = \mathbf{H}\mathbf{x} + \mathbf{n}$. Here $\mathbf{H}$ is the channel matrix of dimension $N_t\times N_r$, and each entry $h_{i,j}$ is the channel gain from transmit antenna i to receive antenna j. All entries in $\mathbf{H}$, $\mathbf{x}$ and $\mathbf{y}$ are complex numbers. The length and direction of the vector representation of the complex number represent the amplitude (or amplitude attenuation) and phase (or phase shift) of the signal, respectively. The environment noise in $\mathbf{n}$ is additive white Gaussian noise (AWGN) with zero mean and variance σ_n^2.

We assume that full channel state information (CSI) is available, *i.e*., each node knows the channel matrices of all adjacent (MIMO) links. A rich-scattering environment is assumed, such that channel matrices are of full rank. PNC-SA is not limited to a particular modulation scheme, and can be adapted to work with all common schemes such as BPSK, QPSK, and QAM 16.

The *trace* of a matrix $\mathbf{A}$ is $Tr(\mathbf{A}) = \sum_i A_{ii}$. $\mathbf{A}^*$ denotes the *conjugate transpose* of a matrix $\mathbf{A}$, obtained by transposing $\mathbf{A}$ first, and then negating the imaginary component of each entry. The *Frobenius norm* of a matrix $\mathbf{A}$ is $\|\mathbf{A}\|_F = (\sum_i \sum_j |A_{ij}|^2)^{\frac{1}{2}} = (Tr(\mathbf{A}^*\mathbf{A}))^{\frac{1}{2}}$. The *Euclidean norm* of a vector $\mathbf{v}$ is $\|\mathbf{v}\| = (\sum_i |v_i|^2)^{\frac{1}{2}}$. A matrix $\mathbf{A}$ is a *unitary matrix* if it satisfies $\mathbf{A}^* = \mathbf{A}^{-1}$. A unitary matrix $\mathbf{A}$ preserves the Frobenium norm, *i.e*., $\|\mathbf{AB}\|_F = \|\mathbf{B}\|_F$.

Throughput this paper, matrices are denoted with boldface capital letters, vectors with boldface lowercase letters, and scalars with non-boldface letters.

IV. A Detailed PNC-SA Scheme Design

We now present a detailed PNC-SA solution design, with reference to the uplink in Fig. 2 for ease of exposition. Applications of PNC-SA elsewhere share a similar workflow. In particular, we study SNR-maximizing precoding at sender side, and tailored detection and decoding algorithms at receiver side. The BER performance will be analyzed in Sec. V.

A. PNC-SA Precoding at Clients

Recall the PNC-SA scheme in Fig. 2. Let $\mathbf{v_1}$ and $\mathbf{v_2}$ be two 2×1 vectors that denote the target directions at AP1 for signal alignment. We have the following *alignment constraint*:

$$\mathbf{H_{11}a_1} = \mathbf{H_{21}a_3} = \mathbf{v_1}, \quad \mathbf{H_{11}a_2} = \mathbf{H_{21}a_4} = \mathbf{v_2}$$

Another type of constraint in PNC-SA comes from the power budget available at each client, E_T. Let $\mathbf{A_1} = (\mathbf{a_1}, \mathbf{a_2})$ and $\mathbf{A_2} = (\mathbf{a_3}, \mathbf{a_4})$ be the 2×2 precoding matrices at clients 1 and 2 respectively. The *nodal power constraint* requires:

$$\|\mathbf{A_1}\|_F^2 = Tr(\mathbf{A_1^*A_1}) \le E_T,$$

$$\|\mathbf{A_2}\|_F^2 = Tr(\mathbf{A_2^*A_2}) \le E_T.$$

Optimal PNC-SA Precoding: Formulation

Given the two types of constraints, the client-side precoding aims to maximize the SNR of x_1+x_3 and x_2+x_4, for demodulation at AP1, leading to the following optimal PNC-SA precoding problem:

$$\text{Maximize} \qquad f(\mathbf{V}) = |\mathbf{v_1^\dagger} \cdot \mathbf{v_2}| \qquad (1)$$

Subject to:

$$\begin{cases} \mathbf{H_{11}A_1} = \mathbf{V} = \mathbf{H_{21}A_2} & (2) \\ \|\mathbf{A_1}\|_F^2 \le E_T & (3) \\ \|\mathbf{A_2}\|_F^2 \le E_T & (4) \end{cases}$$

Here $\mathbf{v_1}^\dagger$ is an orthogonal vector to $\mathbf{v_1}$ with equal length: if $\mathbf{v_1} = (c_1, c_2)^T$, then $\mathbf{v_1^\dagger} = (c_2^*, -c_1^*)^T$, and $\mathbf{v_1} \cdot \mathbf{v_1^\dagger} = 0$. The inner product $f(\mathbf{V}) = |\mathbf{v_1^\dagger} \cdot \mathbf{v_2}|$ targets two goals. The first is maximizing $|\mathbf{v_1}|$ and $|\mathbf{v_2}|$, for large received signal strength at AP1. The second is to make $\mathbf{v_1}$ and $\mathbf{v_2}$ as orthogonal as possible. The two goals together help maximize the SNR of detecting x_1+x_3 and x_2+x_4.

PNC-SA Precoding: Solution

Solving the vector programming problem in (1) is in general computationally expensive [12], especially when the number of antennas is large. In particular, the classic water filling approach [1] does not directly apply, due to the extra alignment constraints in (2). We design an efficient approximate solution instead, which leads to a closed-form representation of the precoding scheme, and becomes optimal with two reasonable restrictions on the precoding space.

Consider the following refinements on the precoding space: (a) $\mathbf{v_1}$ and $\mathbf{v_2}$ are orthogonal. Having orthogonal signals for x_1+x_3 and x_2+x_4 is in general beneficial to their detection; (b) $\|\mathbf{v_1}\| = \|\mathbf{v_2}\|$. This is also reasonable, assuming information contained in x_1+x_3 and in x_2+x_4 are equally important.

Given (a) and (b) above, $\mathbf{V}$ can be scaled to a unitary matrix with total power of 2. We compute how much power is required at each client, for its transmitted signals to fade into a unitary $\mathbf{V}$ at AP1. The power required at client 1 is:

$$\|\mathbf{A_1}\|_F^2 = \|\mathbf{H_{11}^{-1}V}\|_F^2$$

Since $\mathbf{V}$ is unitary, it preserves the Frobenius norm of $\mathbf{H_{11}^{-1}}$, hence $\|\mathbf{A_1}\|_F^2 = \|\mathbf{H_{11}^{-1}}\|_F^2$. This significantly simplifies the precoding design, by decoupling joint precoding at both clients to independent precoding at each of them. Similarly, the power required at AP2 is $\|\mathbf{A_2}\|_F^2 = \|\mathbf{H_{21}^{-1}}\|_F^2$. Let

$$\xi = \max(\|\mathbf{H_{11}^{-1}}\|_F^2), \|\mathbf{H_{21}^{-1}}\|_F^2),$$

we can set the precoding matrices by first picking an arbitrary unitary matrix $\mathbf{V}$, and then set:

$$\mathbf{A_1} = \sqrt{\frac{E_T}{\xi}}\mathbf{H_{11}^{-1}V}, \mathbf{A_2} = \sqrt{\frac{E_T}{\xi}}\mathbf{H_{21}^{-1}V}.$$

The solution above satisfies both the alignment constraint in (2), and the power constraints in (3)-(4) (at least one of them is tight), and maximizes the objective function in (1) under the two simplifying assumptions in (a) and (b).

B. PNC-SA Demodulation at AP1

The digital packets x_1+x_3 and x_2+x_4 are demodulated at AP1 in two steps. Assuming BPSK modulation (+1 for 1, −1 for 0) at the clients, AP1 first detects ternary values in $\{-2, 0, +2\}$, then maps them to binary values in $\{0, 1\}$ through PNC mapping. We next discuss two detection schemes, ZF and ML, followed by PNC mapping.

ZF Detection. Conceptually, AP1 can view x_1+x_3 and x_2+x_4 as two variables, and solve them through the two received signals at its antennas. ZF detection does so by projecting the combined signals to a direction orthogonal to x_2 (x_1), for detecting x_1 (x_2). ZF is particularly well-suited for PNC-SA, if we have restricted $\mathbf{v_1}$ and $\mathbf{v_2}$ to be orthogonal, as described in Sec. IV-A. The ZF projection matrix is a scaled conjugate transpose of $\mathbf{V}$ selected in Sec. IV-A, $\sqrt{\frac{\xi}{E_T}}\mathbf{V}^*$:

$$\begin{aligned} \tilde{\mathbf{y}} &= \sqrt{\frac{\xi}{E_T}}\mathbf{V}^*\mathbf{y} \\ &= \sqrt{\frac{\xi}{E_T}}\mathbf{V}^*(\mathbf{H_{11}A_1}\begin{pmatrix} x_1 \\ x_2 \end{pmatrix} + \mathbf{H_{21}A_2}\begin{pmatrix} x_3 \\ x_4 \end{pmatrix} + \mathbf{n}) \\ &= \sqrt{\frac{\xi}{E_T}}\mathbf{V}^*\left(\sqrt{\frac{E_T}{\xi}}\mathbf{V}\begin{pmatrix} x_1 \\ x_2 \end{pmatrix} + \sqrt{\frac{E_T}{\xi}}\mathbf{V}\begin{pmatrix} x_3 \\ x_4 \end{pmatrix} + \mathbf{n}\right) \\ &= \begin{pmatrix} x_1 \\ x_2 \end{pmatrix} + \begin{pmatrix} x_3 \\ x_4 \end{pmatrix} + \sqrt{\frac{\xi}{E_T}}\mathbf{V}^*\mathbf{n} \\ &= \begin{pmatrix} x_1 + x_3 \\ x_2 + x_4 \end{pmatrix} + \tilde{\mathbf{n}} \end{aligned}$$

Since the projection is linear, the projected noise $\tilde{\mathbf{n}} = \sqrt{\frac{\xi}{E_T}}\mathbf{V}^*\mathbf{n}$ is still AWGN.

ML Detection. Alternatively, we can apply the *a posteriori* method of ML detection. ML infers which source vector is mostly likely to have been transmitted, based on receiver side information. ML has a higher computational complexity than ZF, but provides optimal BER performance.

A salient difference between a standard ML scheme and ML for PNC-SA is that, the former 'guesses' what's transmitted at each send antenna, while the latter 'guesses' the most probable linear combinations of the transmitted data. Equivalently, ML for PNC-SA views the multi-user MIMO channel from both clients to AP1 as a *virtual* 2×2 MIMO channel, with channel matrix $\sqrt{\frac{E_T}{\xi}}\mathbf{V}$ and ternary modulation, and detects the desired linear combination as:

$$\begin{pmatrix} x_1 + x_3 \\ x_2 + x_4 \end{pmatrix} = \arg\min_{\mathbf{x}\in\{-2,0,2\}^2}\|\mathbf{y} - \sqrt{\frac{\mathbf{E_T}}{\xi}}\mathbf{Vx}\|$$

PNC Mapping. While BPSK demodulation simply maps from $\{-1, 1\}$ to $\{0, 1\}$, PNC demodulation maps from $\{+2, 0, -2\}$ to $\{0, 1\}$ [3]. The basic rule is: $+2$ and -2 map to 0, and 0 maps to 1. The intuition is that when $+2$ (-2) is seen, x_1 and x_3 (or x_2 and x_4) must have both been $+1$ (-1), and x_1+x_3 (or x_2+x_4) should be 0. Otherwise x_1+x_3 (or x_2+x_4) should be 1. In the case of ZF detection, one may merge the ternary detection and ternary-to-binary mapping into a single step. Based on a maximum posterior probability criterion, Zhang and Liew [3] derived the following optimal decision rule for such direct mapping: map values between $-1-\alpha$ and $1+\alpha$ to 1, and other values to 0, for $\alpha = \frac{\sigma_n^2}{2}\ln(1+\sqrt{1-e^{-4/\sigma_n^2}})$.

C. PNC-SA Decoding at AP2

After receiving x_1+x_3 and x_2+x_4 from AP1, AP2 has accumulated four packets, two digital ones from AP1, two

analog ones from its own antennas:

$$\begin{cases} \begin{pmatrix} x_1+x_3 \\ x_2+x_4 \end{pmatrix} \\ \mathbf{y'} = \mathbf{H_{12}A_1}\begin{pmatrix} x_1 \\ x_2 \end{pmatrix} + \mathbf{H_{22}A_2}\begin{pmatrix} x_3 \\ x_4 \end{pmatrix} + \mathbf{n} \end{cases}$$

AP2 uses these four packets to decode x_1, x_2, x_3 and x_4. How does AP2 solve the four equations? We describe two approaches below, adapted ML decoding, and decoding via remodulation. The former provides better BER performance, while the latter scales better with the source symbol space and the number of antennas.

Adapted ML Decoding. The ML method can be adapted for decoding at AP2. AP2 traverses all possible combinations of (x_1, x_2, x_3, x_4). Before applying the normal min-distance criterion in ML, it first filters out the enumerated vectors that are not in agreement with the known values for x_1+x_3 and x_2+x_4. Consequently, adapted ML reduces the computational complexity of ML by a factor of 2^{N_r}, or a factor of 4 for the uplink in Fig. 2.

Decoding via Remodulation. Alternatively, AP2 may first re-construct the analog version of x_1+x_3 and x_2+x_4 after modulation. Next, AP2 can apply low-complexity MIMO decoding methods (*e.g.*, ZF or MMSE-SIC [1]) to decode $x_1, \ldots, x_4$ as at a 4×4 MIMO receiver. The IC technique, as in IAC, is essentially decoding via remodulation in its simplest form, where only subtracting the remodulation of an uncoded packet is performed.

D. Discussions

PNC-SA provides full flexibility in precoding. Unlike IA or IAC, it places no restrictions on the precoding matrix, except that each sender can only encode locally available data. PNC-SA also opens new solution spaces for fully exploring the spatial diversity of a MIMO network, augmenting its achievable capacity region. This will be further demonstrated in Sections VI-A, VI-B and VI-C. PNC alone can be viewed as a special case of PNC-SA, where each node has a receive diversity of 1, and SA degrades into signal synchronization. IAC can be viewed as a special case of PNC-SA, which further restricts the way SA is performed, precludes the application of PNC demodulation, and applies decoding via remodulation in its simplest form only.

The technique of PNC-SA is independent of the modulation scheme. We have referred to BPSK for ease of exposition. Similar to PNC [3], PNC-SA can be applied with more sophisticated modulation schemes such as QPSK or QAM 16.

The precoding optimization in Sec. IV-A in general under-utilizes the available power at one of the clients, for exact signal matching between x_1 (x_2) and x_3 (x_4). It is possible to relax exact matching, and fully utilize all available power. An adapted PNC detection scheme will be required, with 4 instead of 3 possible values for combined signal strength. The current precoding optimization focuses on SNR at AP1 only. As a more comprehensive solution, one may formulate a global optimization that further considers the signal reception at AP2. We leave such a formulation and its solution as future work.

V. BER Analysis and Comparison

In this section, we analyze the BER performance of PNC-SA, and compare it with IAC. We first review the BER analysis of a general ML decoder, which will be helpful in analyzing the BER of PNC-SA and IAC.

A. BER of ML Detection

Consider a $N_t \times N_r$ MIMO channel. ML Detection searches for a source vector that was most likely to have been transmitted, based on information available at the receiver side:

$$\tilde{\mathbf{x}}_{\mathbf{ml}} = \arg\max_{\tilde{\mathbf{x}}_\mathbf{i}} p(\mathbf{y}|\mathbf{H}, \tilde{\mathbf{x}}_\mathbf{i}) = \arg\min_{\tilde{\mathbf{x}}_\mathbf{i}} \|\mathbf{y} - \mathbf{H}\tilde{\mathbf{x}}_\mathbf{i}\|^2$$

where the search space of the $N_t \times 1$ source vector $\tilde{\mathbf{x}}_\mathbf{i}$ has a size of M^{N_t}, M being the modulation alphabet cardinality. For flat Rayleigh fading with AWGN, the pairwise error probability (PEP), *i.e.*, the probability that MLD mistakenly outputs $\tilde{\mathbf{x}}_\mathbf{k}$ when a different source vector $\tilde{\mathbf{x}}_\mathbf{i}$ is transmitted, is

$$Pr(\tilde{\mathbf{x}}_\mathbf{i} \to \tilde{\mathbf{x}}_\mathbf{k}) = Q\left(\sqrt{\frac{\|\mathbf{H}(\tilde{\mathbf{x}}_\mathbf{i} - \tilde{\mathbf{x}}_\mathbf{k})\|^2}{2\sigma_n^2}}\right) \qquad (5)$$

Here d_{ik} is the Euclidean distance between $\tilde{\mathbf{x}}_\mathbf{i}$. Function Q computes the area under the tail of a Gaussian PDF. Using Boole's inequality, one can derive the average MIMO vector error probability:

$$Pr_s \le \frac{1}{M^{N_t}} \sum_{\tilde{\mathbf{x}}_\mathbf{i}} \sum_{\tilde{\mathbf{x}}_{k \ne i}} Pr(\tilde{\mathbf{x}}_\mathbf{i} \to \tilde{\mathbf{x}}_\mathbf{k}), \qquad (6)$$

and, an approximation on BER can be found with

$$Pr_b \approx Pr_s/(N_t \log_2 M). \qquad (7)$$

B. BER Analysis of PNC-SA

The analysis of the BER performance of PNC-SA involves two phases. In phase one, we study the BER at AP1, for decoding x_1+x_3 and x_2+x_4. In phase two, we study the BER at AP2, using adapted ML for decoding $x_1, \ldots, x_4$.

BER at AP1. As discussed in Sec. IV-B, AP1 can demodulate x_1+x_3 and x_2+x_4 by applying ML detection over a virtual 2×2 MIMO channel. Let $\mathbf{c} = (c_t, c_b)^T$, where $c_t = x_1 + x_3$ and $c_b = x_2 + x_4$ are in the $\{-2, 0, 2\}$ domain, before PNC mapping. Let $\mathbf{c_i}$ and $\mathbf{c_k}$ be two possible 2×1 transmit vectors, with $i, k \in \{1, \ldots, 9\}$. Assume $\mathbf{c_i}$ is transmitted, from (5), the probability that AP1 incorrectly outputs $\mathbf{c_k}$ is:

$$\begin{aligned} Pr(\mathbf{c_i} \to \mathbf{c_k}) &= Q\left(\sqrt{\frac{d_{ik}^2}{2\sigma_{PNC-SA}^2}}\right) \\ &= Q\left(\sqrt{\frac{\|E_T/\varepsilon\|\mathbf{V}\|^2\lambda_{ik}}{2\sigma_n^2}}\right) = Q\left(\sqrt{\frac{\lambda_{ik}\rho}{2}}\right), \end{aligned}$$

where $\lambda_{ik} = (\mathbf{c_i} - \mathbf{c_k})^T(\mathbf{c_i} - \mathbf{c_k})$, and ρ is SNR per receive antenna.

Let's define constellation points $\mathbf{c_1}, \ldots, \mathbf{c_9}$ as shown in Fig. 3. Assuming 0 and 1 are equally likely to appear in the source packets, the ternary values in $\{-2, 0, 2\}$ appear

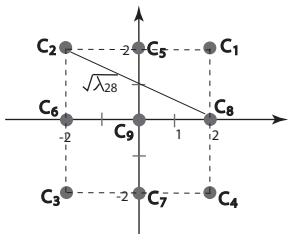

Fig. 3. Constellation diagram for PNC-SA, at AP1.

in $\mathbf{c}$ with probabilities of: $-2:25\%$, $0:50\%$, $2:25\%$. As a result, $P(\mathbf{c_1}) = P(\mathbf{c_2}) = P(\mathbf{c_3}) = P(\mathbf{c_4}) = 1/12$; $P(\mathbf{c_5}) = P(\mathbf{c_6}) = P(\mathbf{c_7}) = P(\mathbf{c_8}) = 1/8$. AP1 wishes to demodulate the digital bits $\mathbf{d} = (d_t, d_b)^T$, where $d_t = x_1 + x_3$ and $d_b = x_2 + x_4$. Thus, $Pr(\mathbf{c_i} \to \mathbf{c_k}) = 0$ when both $\mathbf{c_i}$ and $\mathbf{c_k}$ are in $(\pm 2, \pm 2)^T$. In other words, judging -2 to be $+2$ or vice versa does not lead to an error in $\mathbf{d}$. The average vector error probability for $\mathbf{d}$ is

$$Pr_s(\mathbf{d}) = 4P(\mathbf{c_1}) \sum_{i=5}^{9} Pr(\mathbf{c_1} \to \mathbf{c_i}) +$$

$$4P(\mathbf{c_5}) \sum_{i \neq 5} Pr(\mathbf{c_5} \to \mathbf{c_i}) + P(\mathbf{c_9}) \sum_{i=1}^{8} Pr(\mathbf{c_9} \to \mathbf{c_i})$$

BER at AP2. Consider applying adapted ML to decode $x_1, \ldots, x_4$ at AP2. We first study the case that x_1+x_3 and x_2+x_4 from AP1 are correct. We only need to search over source vectors that agree with the given x_1+x_3 and x_2+x_4 values. Under BPSK modulation, there are 4 such vectors, with dimension 4×1. Let $\tilde{\mathbf{x}}_\mathbf{i}$ and $\tilde{\mathbf{x}}_\mathbf{k}$ $(i, k \in \{1, \ldots, 4\})$ be two distinct vectors among the four. Assume $\tilde{\mathbf{x}}_\mathbf{i}$ is transmitted. By (5), the probability that AP2 outputs $\tilde{\mathbf{x}}_\mathbf{k}$ erroneously equals

$$Pr(\tilde{\mathbf{x}}_\mathbf{i} \to \tilde{\mathbf{x}}_\mathbf{k} | \mathbf{d}_c) = Q\left(\sqrt{\frac{\lambda'_{ik}\rho}{2}}\right).$$

Here $\lambda'_{ik} = (\tilde{\mathbf{x}}_\mathbf{i} - \tilde{\mathbf{x}}_\mathbf{k})^T(\tilde{\mathbf{x}}_\mathbf{i} - \tilde{\mathbf{x}}_\mathbf{k})$. Let $\mathbf{d}_c$ and $\mathbf{d}_w$ denote the events that AP2 gets the correct and wrong data in $\mathbf{d}$ from AP1, respectively. The average vetor error probability is

$$Pr_s(\tilde{\mathbf{x}}|\mathbf{d}_c) = \frac{1}{4} \sum_{i=1}^{4} \sum_{k=1 k \neq i}^{4} Q\left(\sqrt{\frac{\lambda'_{ik}\rho}{2}}\right).$$

Further including the case that x_1+x_3 and x_2+x_4 transmitted from AP1 contain errors, we have $Pr_s(\tilde{\mathbf{x}}) = Pr_s(\tilde{\mathbf{x}}|\mathbf{d}_c)Pr_s(\mathbf{d}_c) + Pr_s(\tilde{\mathbf{x}}|\mathbf{d}_w)Pr_s(\mathbf{d})$. When information from AP1 is wrong, AP2 outputs a wrong vector with probability 1, *i.e.*, $Pr_s(\tilde{\mathbf{x}}|\mathbf{d}_w) = 1$. Therefore the vector error rate of the overall PNC-SA scheme is

$$Pr_s(\tilde{\mathbf{x}}) = Pr_s(\tilde{\mathbf{x}}|\mathbf{d}_c)(1 - Pr_s(\mathbf{d})) + Pr_s(\mathbf{d}). \qquad (9)$$

Since the probability of more than two bits errors happening in the same vector is rather small, we ignore such probabilities.In adapted ML decoding, two of four bits will be decided correctly in each vector, no matter whether AP2 has received the correct combination of (x_1+x_3, x_2+x_4) or not. Thus, the average bit error probability is half the vector error probability. Now we can approximate the BER from the vector error rate:

$$Pr_b(\tilde{\mathbf{x}}) = Pr_s(\tilde{\mathbf{x}})/2. \qquad (10)$$

C. BER Analysis of IAC

The analysis of BER performance for IAC is also carried out in two steps (at AP1 and AP2), similar to the case of PNC-SA in Sec. V-B.

BER at AP1 with ML detection.
With ML, AP1 can decode x_1 and x_2+x_3 simultaneously. Let $\mathbf{e}$ be the spatial source vector with $\mathbf{e} = (e_t, e_b)^T$. There are six possible vectors: $\mathbf{e_1} = (1,2)^T, \mathbf{e_2} = (1,0)^T, \mathbf{e_3} = (1,-2)^T, \mathbf{e_4} = (-1,2)^T, \mathbf{e_5} = (-1,0)^T, \mathbf{e_6} = (-1,-2)^T$. Assume $\mathbf{e_i}$ is transmitted, the probability that AP1 makes a wrong decision in favor of $\mathbf{e_k}$ $(k \neq i)$ equals

$$Pr(\mathbf{e_i} \to \mathbf{e_k}) = Q\left(\sqrt{\frac{d_{ik}^2}{2\sigma_{IAC}^2}}\right) = Q\left(\sqrt{\frac{\lambda_{ik}\rho}{2}}\right).$$

Here $\lambda_{ik} = (\mathbf{e_i} - \mathbf{e_k})^T(\mathbf{e_i} - \mathbf{e_k})$. IAC only utilizes information in x_1. The BER of x_1 is:

$$\begin{aligned} Pr_b(x_1) &= Pr_s(x_1) = 4P(\mathbf{e_1}) \sum_{i=4}^{6} Pr(\mathbf{e_1} \to \mathbf{e_i}) \\ &+ 2P(\mathbf{e_2}) \sum_{i=4}^{6} Pr(\mathbf{e_2} \to \mathbf{e_i}). \end{aligned}$$

BER at AP2. After subtracting x_1 from its received signals, AP2 has two equations for x_2 and x_3. It can then decode x_2 and x_3 using ML detection. Let x_{1_c} and x_{1_w} denote the events that AP2 receives correct and wrong data in x_1 from AP1, respectively. If x_1 from AP1 is correct, the vector error rate at AP2 is:

$$Pr_s(AP2|x_{1\_c}) = \frac{1}{4} \sum_{i=1}^{4} \sum_{k=1 k \neq i}^{4} Q\left(\sqrt{\frac{\lambda'_{ik}\rho}{2}}\right),$$

where ρ is SNR, $\lambda'_{ik} = (\tilde{\mathbf{x}}_\mathbf{i} - \tilde{\mathbf{x}}_\mathbf{k})^T(\tilde{\mathbf{x}}_\mathbf{i} - \tilde{\mathbf{x}_\mathbf{k}})$, $\tilde{\mathbf{x}}_\mathbf{i}$ and $\tilde{\mathbf{x}}_\mathbf{k}$ are two possible spatial source vectors and $i, k \in \{1, \ldots, 4\}$.

There are two sources of BER in IAC. First, BER under event x_{1_c} can be calculated from the vector error rate directly.

$$\begin{aligned} Pr_b(x)_1 &= Pr_s(x)_1/N_t \log_2^M = Pr_s(AP2|x_{1\_c})Pr_s(x_{1\_c})/2 \\ &= Pr_s(AP2|x_{1\_c})(1 - Pr_s(x_1))/2. \end{aligned}$$

Second, when x_1 from AP1 is incorrect, the output of (x_2, x_3) at AP2 is almost surely wrong, due to error propagation. In other words,

$$Pr_b(x)_2 = Pr_s(x)_2 = Pr_s(AP2|x_{1\_w})Pr_s(x_{1\_w}) = Pr_s(x_1).$$

Now, the overall BER of the IAC scheme can then be approximated as: $Pr_b(x) = Pr_b(x)_1 + Pr_b(x)_2$.

D. Comparison of BER Performance

Fig. 4 shows the comparison of the BER performance of PNC-SA and IAC, as computed in Sec. V-B and Sec. V-C, under varying SNR levels. We can observe that the BER of PNC-SA is rather close to yet slightly better than that of IAC, under the same SNR at the receiver's antennas.

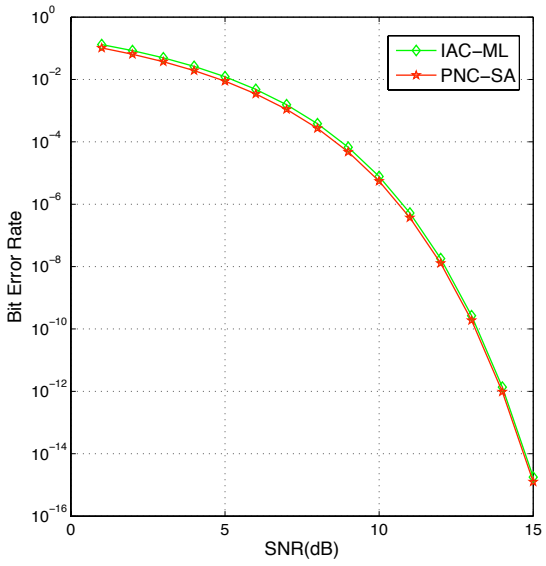

Fig. 4. BER performance comparison: PNC-SA *vs* IAC.

VI. General Applications of PNC-SA and Packet-level Throughput

Applications of PNC-SA in wireless routing are diverse, and are not restricted to cases where receivers have limited collaboration (Fig. 2). In this section, we first present simulation results on packet level comparisons between PNC-SA and alternative solutions for the uplink scenario in Fig. 2. We then extend the discussions to more general applications of PNC-SA, for information exchange, unicast and multicast/broadcast.

Fig. 5 shows the comparison of packet-level throughput achieved by PNC-SA, IAC and MIMO, respectively. In the simulations, we assume a synchronized environment where the nodes transmit packets in rounds. For this first set of simulations we let the system run for 100 rounds. During each round, each node transmits 1 packet of length 50 bits. Consequently, in each round, PNC-SA, IAC and MIMO transmit 4, 3, and 2 raw packets, respectively. On the receiver side, we assume the existence of an error detection scheme that can identify bit errors. A packet received with 1 or more bits in error is discarded and not counted towards total throughput. The bit errors are computed from SNR as discussed in Sec. V. The SNR level is assumed to be equal at all nodes.

From Fig. 5, we can see that at high SNR (> 9), the ratio of throughput achieved by the three schemes converges to $4:3:2$, with PNC-SA performing the best. The case of low SNR does not follow the same trend though. It is interesting to note that basic MIMO actually performs the best at low SNR here, due to its better SNR-BER performance.

A. PNC-SA for Info Exchange

Fig. 6 shows the well-known Alice-and-Bob communication scenario in a wireless network, where Alice and Bob wish to exchange data packets with the help of a relay [11], [13].

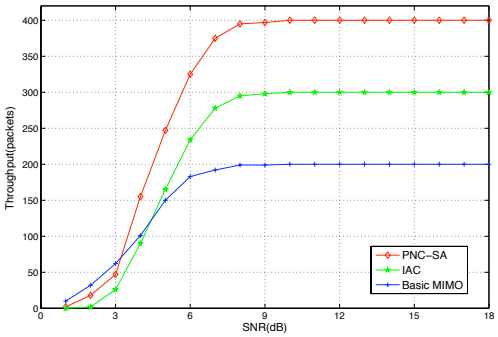

Fig. 5. Packet-level throughput for multi-AP uplink communication, PNC-SA *vs*. IAC *vs*. MIMO alone.

Each node is equipped with 3 antennas. Transmitting simultaneously, Alice and Bob can align their six signals to three common directions at the relay. The relay then demodulates x_1+x_4, x_2+x_5 and x_3+x_6, and broadcasts them to both Alice and Bob. Alice and Bob each subtract their known packets from the three combined signals received, and apply normal demodulation to recover the other three packets.

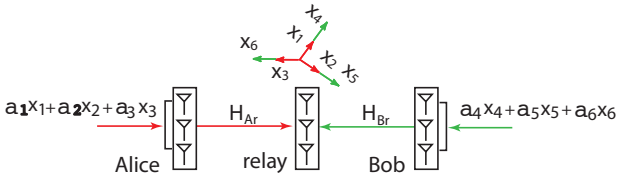

Fig. 6. PNC-SA with three antennas per node. Here and in the rest of the paper, we label an aligned direction with the corresponding signal instead of its vector direction, for simplicity. For example, the direction of $\mathbf{H_{11}a_1}$ is simply labelled as x_1.

With PNC-SA, 6 packets can be exchanged in 2 time slots. Without PNC-SA, it takes 3 time slots with digital network coding, and 4 time slots with no coding at all [13]. Without SA, PNC alone does not fully exploit the full degree of freedom of such a MIMO network. For example, Zhang and Liew [11] studied the utilization of multiple antennas at the relay, by combining its received signals for generating a single encoded packet, for better BER.

We can see that the application of PNC-SA is not limited to scenarios with limited receiver collaboration; nor is it limited to 2 antennas per node. Examples shown in this paper can all be generalized to work with 3 or more antennas per node.

Fig. 7 shows the packet-level throughput comparison between PNC-SA, DNC and basic MIMO. Here the system is run for 200 time slots, during each of which a node can transmit 1 packet of 50 bits. We can observe that at high SNR, the throughput ratio converges to $6:4:3$, with PNC-SA leading the alternatives. At low SNR, DNC performs the worst. The main reason is that DNC needs to succeed in all transmissions in 3 time slots for successful packet reception and decoding, while PNC-SA and MIMO only need 2 time slots each.

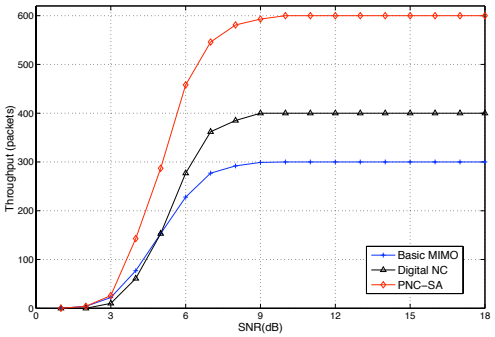

Fig. 7. Packet-level throughput for information exchange, PNC-SA *vs*. DNC *vs*. MIMO alone.

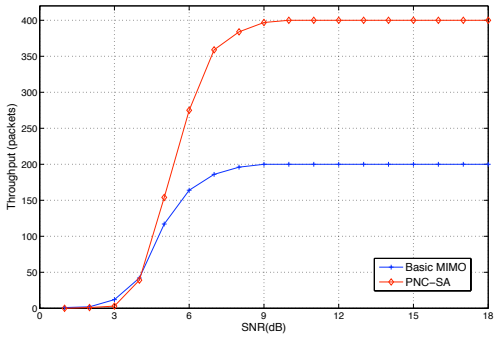

Fig. 9. Packet-level throughput for cross unicasts, PNC-SA *vs*. MIMO alone.

B. PNC-SA for Unicast Routing

PNC-SA for Cross Unicasts

Fig. 8 depicts two unicast sessions, from S_1 to T_1 and from S_2 to T_2, whose routes intersect at a relay. Each sender can not directly reach its intended receiver, and needs to resort to the help of the relay node in the middle.

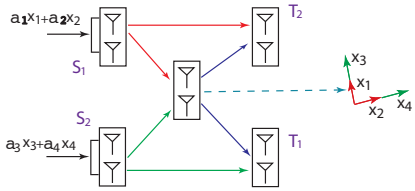

Fig. 8. PNC-SA with PNC performed at the relay node in the middle.

With PNC-SA, the two senders can transmit simultaneously. They align the signals for reception at the relay, such that x_1 is aligned with x_3, and x_2 with x_4. The relay decodes and broadcasts $x_1{+}x_3$ and $x_2{+}x_4$. Only 3 transmissions in 2 time slots are required. T_1 can first decode x_3 and x_4 overhead from S_1, and then combine them with $x_1{+}x_3$ and $x_2{+}x_4$ to recover x_1 and x_2. T_2 recovers x_3 and x_4 similarly.

Without any coding, it takes 4 transmissions in 4 time slots to send 2 packets in each session: each sender transmits once (using both antennas), the relay transmits twice. With DNC, it takes 3 transmissions in 3 time slots — the relay can transmit just once, broadcasting two encoded packets.

The PNC-SA precoding optimization discussed in Sec. IV-A still applies here. SA enables PNC in this MIMO network, and PNC further enables demodulate-and-forward at the relay, which provides an alternative to amplify-and-forward for cooperative communication [14]. In general multi-session unicast routing, such a cross-unicast topology can be applied as a gadget, embedded into larger unicast sessions [13].

Fig. 9 shows packet-level throughput comparison between PNC-SA and a basic MIMO solution. Again the network is run for 200 time slots, with same node transmission capacity and packet lengths as previously assumed. At high SNR, the throughput gap between PNC-SA and MIMO is a factor of 2, confirming the analysis above. As SNR decreases, however, MIMO catches up with PNC-SA and eventually outperforms, due to its better SNR-BER performance. This suggests that a good design of error-correction code in combination with PNC-SA is important at the low SNR regime.

The Zig-Zag Unicast Flow: PNC Meets DNC

Existing literature on the application of network coding in wireless routing often focuses on identifying local gadgets, such as the Alice-and-Bob topology and the cross-unicast topology [3], [13]. These gadgets usually involve multiple unicast sessions with reverse or crossing routes. It is often believed that network coding provides little benefit to a single unicast session with lossless links [15], [16]. We present an application of PNC-SA, where PNC and DNC work in concert to enable a new, efficient wireless unicast routing algorithm.

Consider a large wireless mesh network, with two antennas per sensor. We wish to transfer information from the top of the network to the bottom [17]. What multi-hop unicast routing scheme can we use, to achieve a high throughput? Fig. 10 illustrates a PNC-SA based solution: a *zig-zag unicast flow*.

The zigzag solution routes k parallel data streams side by side, employing k nodes for transmission at each row (k=3 in Fig. 10). The resulting unicast flow exhibits a zigzag topology. The following theorem shows that the packets at each row can be used to recover the $2k$ original packets.

Theorem 7.1. At each row in the zigzag unicast flow, the $2k$ data packets are linearly independent, and can be used to recover the original packets $x_1, \ldots, x_{2k}$.

Proof: We prove the theorem using a row-by-row induction. As the basis, the $2k$ packets at the first row are the original ones, and are independent. Assume the packets at row i, $y_1, \ldots, y_{2k}$, are independent. Number the nodes in each row from left to right. Without loss of generality, assume the left-most node (node 1) in row $i+1$ receives packets without PNC coding. Packets at node 1 in row $i+1$ are y_1 and y_2. Packets at node 2 in row $i+1$ are $y_1{+}y_3$ and $y_2{+}y_4$ and can be used to further recover y_3 and y_4. Similarly, each node $j \in [2 \ldots k]$ in row $i+1$ possess packets that can be used to further recover y_{2j-1} and y_{2j}. In conclusion, packets at row $i{+}1$ can be used to recover all packets in row i. Since the latter are linearly

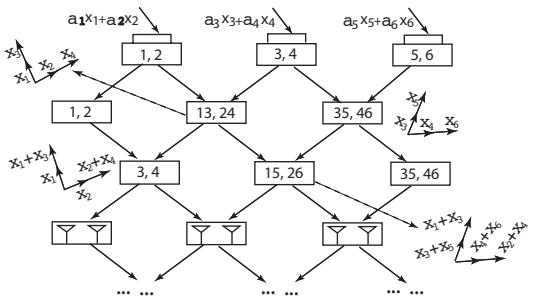

Fig. 10. The zig-zag unicast flow using PNC-SA. Here 35, 46 in a node represents x_3+x_5 and x_4+x_6. The first row transmits 6 packets simultaneously. The signals are aligned at the second row for demodulating (x_5, x_6), (x_3+x_5, x_4+x_6) and (x_1+x_3, x_2+x_4). In the odd (even) number of rows, the left-most (right-most) node receive from one sender in the previous row only, without PNC.

independent, so are the former. □

The table below lists the packets received by nodes at each row, for $k = 3$. The intra-row linear independence can be verified. It is also interesting to observe that after every 7 rows, the 6 data packets in routing return to uncoded form.

row	node 1	node 2	node 3
0	x_1, x_2	x_3, x_4	x_5, x_6
1	x_1, x_2	x_1+x_3, x_2+x_4	x_3+x_5, x_4+x_6
2	x_3, x_4	x_1+x_5, x_2+x_6	x_3+x_5, x_4+x_6
3	x_3, x_4	$x_1+x_3+x_5$, $x_2+x_4+x_6$	x_1+x_3, x_2+x_4
4	x_1+x_5, x_2+x_6	x_5, x_6	x_1+x_3, x_2+x_4
5	x_1+x_5, x_2+x_6	x_1, x_2	$x_1+x_3+x_5$, $x_2+x_4+x_6$
6	x_5, x_6	x_3+x_5, x_4+x_6	$x_1+x_3+x_5$, $x_2+x_4+x_6$
7	x_5, x_6	x_3, x_4	x_1, x_2

Compared to a basic single-chain unicast solution, the zigzag flow represents a $\times k$ throughput gain. Unlike traditional multi-path wireless routing, the k parallel data streams in the zigzag flow do not need to be spatially far apart to avoid interference, and is in that sense more practical to deploy. The rational behind the zigzag structure guarantees that a node at the border obtains data without PNC, which can be used to bootstrap the decoding process among that row.

C. PNC-SA for Multicast Routing

Network coding is naturally well-suited for multicast and broadcast routing in wireless networks. The local broadcast nature of omnidirectional antennas is well suited for simultaneously transmitting an encoded packet to multiple receivers. PNC-SA extends such benefit of DNC to information dissemination in MIMO networks.

Multi-Sender Multicast

Fig. 11 depicts a multi-sender multicast in an 8-node MIMO network. The 3 top nodes are senders, the 3 bottom nodes are receivers. Each sender wishes to multicast to all receivers. As

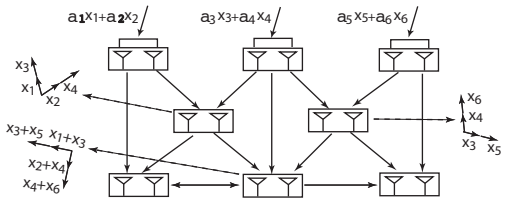

Fig. 11. Multicast from top layer to bottom layer. PNC-SA doubles throughput.

another natural fusion of PNC and DNC, the application of PNC-SA here doubles achievable multicast throughput.

With PNC-SA, 6 packets can be multicast to all receivers in 4 time slots. (i) The three senders align their six signals at the two relays in the middle, such that they can successfully demodulate $\{x_1+x_3, x_2+x_4\}$ and $\{x_3+x_5, x_4+x_6\}$, respectively. At the same time, the three receivers obtain $\{x_1, x_2\}$, $\{x_3, x_4\}$ and $\{x_5, x_6\}$, respectively. (ii) The two relays transmit x_1+x_3, x_2+x_4, respectively, simultaneously. Their signals are aligned so the middle receiver can demodulate $x_1+x_3+x_3+x_5 = x_1+x_5$ and $x_2+x_4+x_4+x_6 = x_2+x_6$. From left to right, the three receivers accumulate $\{x_1, x_2, x_3, x_4\}$, $\{x_3, x_4, x_1+x_5, x_2+x_6\}$ and $\{x_3, x_4, x_5, x_6\}$, respectively. (iii) The middle receiver broadcasts x_1+x_5 and x_2+x_6, the other two receiver can now recover all 6 packets via DNC decoding. (iv) The left receiver transmits x_1 and x_2 to the middle receiver, who can now decode all 6 original packets too.

Using a straightforward multicast scheme without network coding, we need 7 time slots instead. x_1 and x_2 require 3 broadcasts to reach all receivers, the same for x_5 and x_6. x_3 and x_4 require two broadcasts. Among these 8 broadcast transmissions, only two can be scheduled concurrently, resulting in a total of 7 time slots. With DNC, the number of time slots required is between that of PNC-SA and of a no coding solution, at 5.

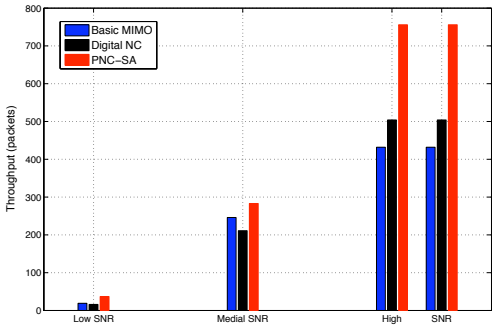

Fig. 12. Packet-level throughput for multicast, PNC-SA *vs*. DNC *vs*. MIMO alone.

Fig. 12 shows packet-level throughput achieved by PNC-SA, DNC and MIMO. The network is simulated for 168 time slots, with identical node transmission capacity and packet length as previously assumed. At high SNR, PNC-SA

again demonstrates a marked throughput gain. DNC slightly leads MIMO at high SNR, but becomes inferior when SNR decreases due to its relatively worse SNR-BER performance.

VII. Conclusion

Signal alignment (SA) was introduced in this paper. We showed that PNC-SA, SA coupled with PNC, can open new design spaces for routing in MIMO wireless networks, and can hence augment the network capacity region. The design of PNC-SA has been inspired by recent advances in PNC and IA research, yet PNC-SA can better exploit the spatial diversity and precoding opportunities of a MIMO network, for achieving higher throughput. We studied the new problem of optimal precoding introduced by PNC-SA, formulated it into a vector programming problem, and designed a solution for maximizing SNR at the receiver. The SNR-BER performance of PNC-SA was then analyzed. General applications of both PNC-SA and SA alone were demonstrated, in various multi-hop MIMO routing scenarios, including information exchange, unicast and multicast. Throughput gain of up to a factor of 2 was observed, compared to simple solutions without coding.

References

[1] D. Tse and P. Viswanath, *Fundamentals of Wireless Communication*. Cambridge, UK: Cambridge University Press, 2005.

[2] S. Gollakota, S. D. Perli, and D. Katabi, "Interference Alignment and Cancellation," in *Proc. of ACM SIGCOMM*, 2009.

[3] S. Zhang, S. C. Liew, and P. P. Lam, "Physical-Layer Network Coding," in *Proceedings of ACM MobiCom*, 2006.

[4] R. Ahlswede, N. Cai, S. R. Li, and R. W. Yeung, "Network Information Flow," *IEEE Transactions on Information Theory*, vol. 46, no. 4, pp. 1204–1216, July 2000.

[5] J. H. Winters, J. Salz, and R. D. Gitlin, "The Impact of Antenna Diversity on the Capacity of Wireless Communication Systems," *IEEE Transactions on Communications*, vol. 42, no. 2, pp. 1740–1751, March 1994.

[6] S. Zhang, S. C. Liew, and P. P. Lam, "On The Synchronization of Physical-Layer Network Coding," in *Proceedings of IEEE Information Theory Workshop (ITW)*, 2006.

[7] V. R. Cadambe and S. A. Jafar, "Interference Alignment and Degrees of Freedom of the K-User Interference Channel," *IEEE Transactions on Information Theory*, vol. 54, no. 8, pp. 3425–3441, August 2008.

[8] L. E. Li, R. Alimi, D. Shen, H. Viswanathan, and Y. R. Yang, "A General Algorithm for Interference Alignment and Cancellation in Wireless Networks," in *Proc. of IEEE INFOCOM*, 2010.

[9] A. Özgür and D. Tse, "Achieving Linear Scaling with Interference Alignment," in *Proceedings of IEEE International Symposium on Information Theory (ISIT)*, 2009.

[10] K. S. Raghupathy, K. Sundaresan, R. Sivakumar, M. A. Ingram, and T. Chang, "A Fair Medium Access Control Protocol for Ad-hoc Networks with MIMO Links," in *Proceedings of IEEE INFOCOM*, 2004.

[11] S. Zhang and S. C. Liew, "Physical-Layer Network Coding with Multiple Antennas," in *CoRR abs/0910.2603*, 2009.

[12] J. Zhan, B. Nazer, M. Gastpar, and U. Erez, "MIMO Computer-and-Forward," in *Proceedings of IEEE International Symposium on Information Theory (ISIT)*, 2009.

[13] S. Katti, H. Rahul, W. Hu, D. Katabi, M. Médard, and J. Crowcroft, "XORs in The Air: Practical Wireless Network Coding," *IEEE/ACM Transactions on Networking*, vol. 16, no. 3, pp. 497–510, June 2008.

[14] A. Scaglione, D. L. Goeckel, and J. N. Laneman, "Cooperative Communications in Mobile Ad Hoc Networks: Rethinking the Link Abstraction," *Distributed antenna systems, Auerbach Publications*, pp. 87–111, 2007.

[15] R. Gummadi, L. Massoulie, and R. Sreenivas, "The Role of Feedback in the Choice between Routing and Coding for Wireless Unicast," in *IEEE Symposium on Network Coding (NetCod)*, 2010.

[16] Z. Li, B. Li, and L. C. Lau, "A Constant Bound on Throughput Improvement of Multicast Network Coding in Undirected Networks," *IEEE Transactions on Information Theory*, vol. 55, no. 3, pp. 997–1015, March 2009.

[17] M. Gastpar and M. Vetterli, "On the capacity of wireless networks: the relay case ," in *Proceedings of IEEE INFOCOM*, 2002.